



Exploring The Potential of Using Discrete Wavelet Transform (DWT) for Heart Sound Analysis

Nadia Muftah Algolaib
Misurata University

Ali M Abdulshahed
Misurata University

Abstract— This paper delves into the effectiveness of the Discrete Wavelet Transform (DWT) in analyzing cardiac sounds, highlighting its benefits, practical applications, and associated challenges. It reviews various DWT-based techniques for preprocessing, feature extraction, and classification of cardiac sounds, emphasizing their success in detecting anomalies and enhancing diagnostic precision. The study showcases DWT's potential as a powerful tool for improving cardiac sound analysis.

The proposed method was evaluated, achieving an accuracy of 84%, with sensitivity ranging from 63% and specificity from 62%. These results underscore the method's reliability in contributing to neural network systems for classifying cardiac sound signals as normal or abnormal. The Adaptive Neuro Fuzzy Inference System (ANFIS), when combined with DWT attributes, emerges as an effective tool, showcasing its capability in the PhysioNet Challenge 2016.

Index Terms— heart sound, discrete wavelet transform, adaptive neuro fuzzy inference system

I. INTRODUCTION

Heart diseases cannot be adequately diagnosed through the analysis of heartbeat sounds by auscultation. This method fails to provide the analyst with both qualitative and quantitative information about the phonocardiogram signals [1,2].

The presence of murmurs and aberrations, caused by various pathological conditions of the cardiovascular system, can be observed in abnormal heartbeat sounds [2]. However, it is evident from the study of the physical characteristics of heart sounds and human hearing that the human ear is ill-suited for cardiac auscultation [3]. Consequently, the ability of clinics to diagnose heart sounds is limited.

Additionally, during a single cardiac cycle, the sound emitted by the human heart consists of two dominant events known as the first heart sound (S1) and the second heart sound (S2). S1 is associated with the closure of the mitral and tricuspid valves, while S2 is produced by the cessation of the aortic and pulmonary valve leaflets [1]. S1 coincides with the timing of the QRS complex in the Electrocardiogram (ECG), and S2 follows the systolic pause in the normal cardiac cycle. Furthermore, the study

of the physical properties of heart sounds and human hearing reveals that the human ear is not well-suited for cardiac auscultation [3].

Compared to the pulmonic component, the aortic component is louder. It can be heard at every auscultation location. As opposed to the pulmonic, which can only be heard at the left base when the diaphragm of the chest piece is firmly pushed, it can be heard the Best at the right base.

Because the aortic valve closes before the pulmonary valve does during typical cardiac activity, the aortic component often has higher frequency contents and occurs before the pulmonary component. In the medical world, the interval in time between these valve activities is referred to as split [4-6] but this order of time occurrence can be reversed and its delay can vary in different disorders [1].

Digital signal processing techniques allow for more exact measurement of the PCG signal's properties as well as other parameters like the position of the heart sounds S1 and S2, the number of components for each sound, their frequency content, and their time interval.

The Fast Fourier Transform (FFT), can give a general idea of the frequency composition of cardiac sounds. If the signal's stationary assumption is broken, however, FFT analysis is still only useful for a restricted range of values. Heart sounds are categorized as non-stationary signals because they show noticeable variations over time and frequency. Studying the time-frequency properties of such signals is crucial in order to comprehend their precise features. This study investigates normal and pathologically abnormal cardiac sounds in both the temporal and frequency domains using wavelet transform. It has been shown that this method offers excellent temporal resolution for high-frequency components. In fact, as the frequency increases, the time resolution improves, and as the frequency decreases, the frequency resolution enhances [4,5]. Additionally, in certain pathological situations, the wavelet transform has proven to be able to evaluate the heart sound more precisely than other methods like STFT or Wigner distribution [6]. In actuality, extremely sensitive abrupt changes in the time direction cannot be tracked by the spectrogram (STFT).

The time frame must be kept as short as feasible in order to appropriately handle these temporal shifts. On the other hand, this will cause the time-frequency plane's frequency resolution to decrease. As a result, time and frequency resolutions are traded off [6]. Nonetheless, in the investigation of non-stationary signals, the Wigner distribution (WD) and the associated WVD (Wigner Ville Distribution) have demonstrated strong performances. This results from the WD's capacity to distinguish signals in both the frequency and temporal domains. The absence of the time-frequency trade-off issue is one benefit of the WD over the STFT. However, because the WD uses cross-terms in its response, it has a drawback. These cross-terms have no physical meaning and are the result of the WD's nonlinear behavior. Smoothing the time-frequency plane is one method of eliminating these cross-terms, although doing so will result in less resolution in both time and frequency [7]. When the WD is applied to a heart sound signal, it fails to separate or display the signal components in both the time and frequency directions [6]. However, in basic monocomponent signal analysis, it offers great time and frequency resolution [8,9]. The wavelet transform (WT) is an alternate method of analyzing non-stationary signals that gets around these issues with the STFT and WD. One method used in the field of time-frequency distributions is the wavelet transform. Based on a dyadic pavement, the representation timing of WT seems more adaptable. It is a mathematical structure where the presence of an orthonormal basis is made feasible by a formula of perfect inversion [10]. As a result, the wavelet becomes a simultaneous function of frequency and time. It has been demonstrated that this transform offers sufficient PCG signal properties to assist clinics in measuring the time-frequency characteristics of the PCG signal both qualitatively and quantitatively, which will ultimately help with diagnosis. This study aims to investigate the effectiveness of utilizing artificial intelligence techniques and wavelet transform in diagnosing cardiac murmurs, which are indicative of underlying heart conditions. Accurate and timely diagnosis is essential for effective cardiovascular disease management [10]. The proposed approach employs artificial intelligence (AI) methods, specifically machine learning (ML), in combination with wavelet transform as a preprocessing technique. Wavelet transform is applied to murmur signals to extract important features, enhancing diagnostic accuracy. The machine learning model is trained using the PhysioNet Challenge 2016 database of simulated cardiac murmurs. The Adaptive Neuro-Fuzzy Inference System (ANFIS) is trained to identify patterns and characteristics related to murmurs, with its classification accuracy being thoroughly assessed.

II. BACKGROUND

A. Heart Sounds

In the intricate cardiovascular system of humans, a typical cardiac cycle comprises of two distinctive heart melodies: the initial heart note S1 and the subsequent heart note S2. Abnormal sounds can serve as red flags for underlying conditions; for instance, a noticeable third heart sound S3 might hint at heart malfunction, whereas a murmur could suggest issues with valves or an opening in the septal barrier [11]. The spectrum of S1 and S2 spans from 20 to 200 Hz, whereas the frequencies of S3 and S4 fall within the range of 15 to 65 Hz [12].

Murmurs, resulting from the turbulent flow of blood within the intricate heart system, serve as distinctive abnormal auditory signals. These sounds play a crucial role in determining the rhythm and tone essential for the detection of cardiovascular ailments [13]. Within the area of medical diagnosis, murmurs often serve as the primary indicator for identifying valvular conditions of the heart [14]. Clinically categorized, murmurs manifest in two forms: systolic murmurs and diastolic murmurs. Systole witnesses the occurrence of aortic stenosis, mitral regurgitation, and tricuspid regurgitation, while diastole presents mitral stenosis and tricuspid stenosis [15].

B. Phonocardiography (PCG)

Furthermore, phonocardiography (PCG) enables the extraction of informative features from heart sounds that are imperceptible to the human ear [19]. Traditional heart auscultation, which relies on brief, stethoscope-assisted listening, is subjective and depends on the physician's expertise in discerning various heart sound patterns [21]. In contrast, PCG provides an objective and standardized assessment method capable of continuously capturing heart sounds, overcoming the limitations of human auditory perception [22]. Therefore, there is a need for more objective tools like PCG to facilitate the examination of heart sounds and cardiac irregularities, thereby enhancing diagnostic efficacy overall.

A typical PCG recording comprises two primary cardiac sounds: the first heart sound (S1) and the second heart sound (S2), which correspond to the closure of the atrioventricular and semilunar valves, respectively [23]. The period from the onset of S1 to the onset of S2 is referred to as the systole interval (S1-S2 interval), while the period from the onset of S2 to the onset of S1 is termed the diastole interval (S2-S1 interval) [24]. The diastole interval is generally longer than the systole interval [25]. The mean duration and frequency range of S1 and S2 are approximately 100 ms and below 180 Hz, respectively [26]. Figure 1 illustrates a phonocardiogram signal displaying normal heart sounds along with S1, S2, systole, and diastole intervals.

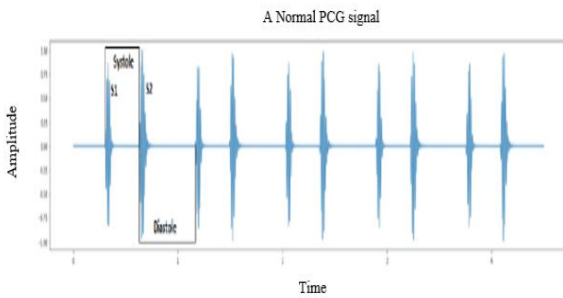


Figure 1. PCG signal of Normal heart sound

Besides S1 and S2, additional cardiac sounds known as the third and fourth heart sounds (S3 and S4) may manifest under various physiological and pathological conditions. S3 typically occurs immediately following S2, while S4 is usually observed just before S1. In addition to these heart sounds, various types of cardiac murmurs may be detected in the signal. These murmurs stem from turbulent blood flow across the valves and are often associated with cardiac pathologies. Delays in the opening or closing of a valve can impede proper blood flow through the heart, leading to compromised circulation or potential overflow, resulting in murmurs. Murmurs may be audible during systole, diastole, or both cardiac intervals, and they typically exhibit higher frequencies (180-400 Hz) compared to the heart sounds. Figure 2 illustrates a phonocardiogram signal featuring murmurs and the third heart sound.

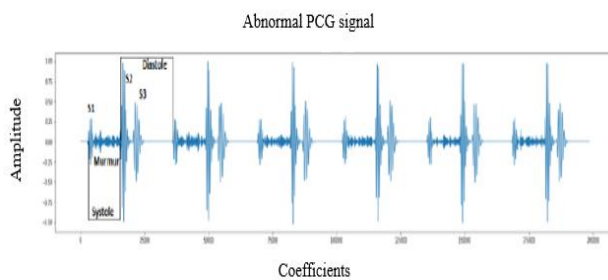


Figure 2. PCG signal with murmurs and S3.

The spatial coordinates, magnitude, and temporal extent of the cardiac sounds, the duration of systole and diastole phases, cardiac cycle, and the heart rate per minute are crucial factors in assessing an individual's cardiac function [27]. Various signal analysis methods commonly employed include Fourier Transform (FT), Short Time Fourier Transform (STFT), and Discrete Wavelet Transform (DWT). While FT and STFT are frequently utilized for analyzing stationary signals, their efficacy diminishes when dealing with non-stationary signals due to the inability to offer simultaneous time and frequency localization [28]. Conversely, DWT exhibits high performance in analyzing non-stationary signals such as Phonocardiogram (PCG) owing to its superior time-frequency localization capabilities and multi-resolution analysis achieved through the utilization of the mother wavelet and windowing technique [29]. Through DWT,

signal decomposition into distinct frequency bands is feasible, enabling the extraction of the desired frequency band for further processing. Consequently, the application of multi-resolution analysis based on DWT aids in eliminating redundant data and noise from the signal, while retaining essential clinical information crucial for diagnosis [30]. The optimal selection of decomposition levels and suitable mother wavelets significantly influences the effectiveness of DWT in signal analysis [31].

C. Discrete Wavelet Transform

The Discrete Wavelet Transform (DWT), as discussed in literature review [32,33], is founded on the principle of sub-band coding, facilitating rapid computation of the Wavelet Transform. Its computational efficiency is evident through reduced time and resource requirements, alongside its ease of implementation. Analysis of signals is conducted by employing a sequence of fundamental functions within the realm of the continuous wavelet transform (CWT), which are interconnected through uncomplicated scaling and translation processes. The mathematical representation of the continuous wavelet transform (CWT) is explicitly formulated as follows:

$$W(a, b) = \int_{-\infty}^{\infty} \chi(t) \frac{1}{\sqrt{a}} \Psi^* \left[\frac{t-b}{a} \right] dt \quad (1)$$

In this context, the variable $\chi(t)$ represents the initial signal, while $\psi(t)$ denotes the wavelet function, with a and b serving as the scaling and displacement factors that define the magnitude and location of the wavelet function.

In the analysis of DWT signals, multiple scales (m) and positions (k) can be selected to integrate wavelets and create a signal at a desired scale. By integrating the signal across all resolutions, the original input signal is obtained. In multilevel analysis, the scale of analysis is reduced by a factor of two. Hence, this represents a DWT-type dyadic wavelet transform, as outlined in "equation (2)," [34].

$$DWT(m, n) = \frac{1}{\sqrt{2^m}} \sum_k f(k) \psi \left[\frac{n-k2^m}{2^m} \right] \quad (2)$$

where

$m, n, k = \text{Integers}$

$\psi = \text{Mother wavelet}$

$n = \text{Number of data points}$

$m = \text{Scaling}$

$k = \text{Shifting}$

Signals are decomposed by the wavelet. The mother wavelet is a filter signal that separates the following two channels:

- High-frequency component (detail coefficient: cD).
- Low-frequency component (approximation coefficient: cA).

The high-frequency component will be used to analyze signal during transient state.

The mother wavelets used in the DWT are db, sym, coif, and bior [35]. Each mother wavelet for discrete-time signals, the discrete wavelet transform (DWT) is known to be a natural wavelet transform. The parameters for time and time-scale are both discrete. The algorithm used to carry out the transformation has an impact on the discretization process [36].

As depicted in Figure 2, the discrete time-domain signal undergoes successive low-pass and high-pass filtering to generate the DWT. The utilization of the Mallat algorithm, also referred to as the Mallat-tree decomposition, is employed for this purpose. The half band filters exclusively yield signals that encompass a portion of the frequency spectrum at each stage of disintegration. Consequently, the frequency uncertainty is halved, thereby enhancing the frequency resolution by a factor of two. According to the Nyquist rule, if the highest frequency of the original signal was denoted as ω , and the sampling frequency was 2ω radians, the outcome is that the highest frequency of the signal is now reduced to $\omega/2$ radians. Consequently, the signal can be sampled at a frequency of ω , allowing for the rejection of half the samples devoid of information. Due to the two-fold reduction, the time resolution is diminished by half as only half the number of samples are utilized to represent the entire signal. In contrast to the half-band low pass filtering, which reduces frequencies by half, and reduces resolution by the same amount, decimation by two increases scale.

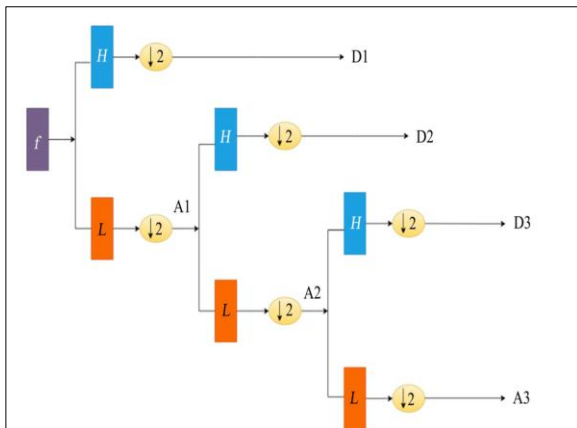


Figure 3. Decomposition tree of level 3.

Up until the target level is obtained, the filtering and decimation process is repeated. The maximum number of levels is determined by the signal length. Next, starting with the last level of decomposition, all the coefficients, approximations, and details are concatenated to produce the DWT of the original signal.

The discrete wavelet transform (DWT), a quick and effective algorithm for computing the wavelet transform of a discrete-time signal, is one of the most frequently used wavelet transforms. A signal is broken down by the DWT into a collection of wavelet coefficients at various scales and locations which can then be used to rebuild the original signal. The formula is defined as follows:

$$C_{j,k} = \langle x, \psi_{j,k} \rangle = \frac{1}{\sqrt{2^j}} \sum_{n=0}^{N-1} x[n] \psi_{j,k} [n] \quad (3)$$

the original signal x is decomposed by the Discrete Wavelet Transform (DWT) into a collection of coefficients $C_{j,k}$. These coefficients enable the reconstruction of the initial signal through the application of the inverse discrete wavelet transform. The wavelet function $\psi_{j,k}$ represents the function at scale j and translation k , with N denoting the signal's length.

III. MATERIALS AND METHOD

A. Signal Decomposition (DWT)

The utilization of a pair of uncomplicated low pass and high pass filters allows for the implementation of the scaling function and wavelet functions. Upon considering the filters with their impulse responses represented as $\{H(n), n \in \mathbb{N}\}$ for the low pass filter and $\{G(n), n \in \mathbb{N}\}$ for the high pass filter, the signal's decomposition through Discrete Wavelet Transform (DWT) can be depicted as illustrated in Figure (6). This particular decomposition is commonly referred to as dyadic decomposition. In the initial stage, the frequency spectrum is bifurcated into two identical parts (low pass and high pass). Subsequently, the second stage further divides the low pass band into an additional low pass band and high pass band. This process continues with the second stage dividing the lower half into quarters and so forth [41].

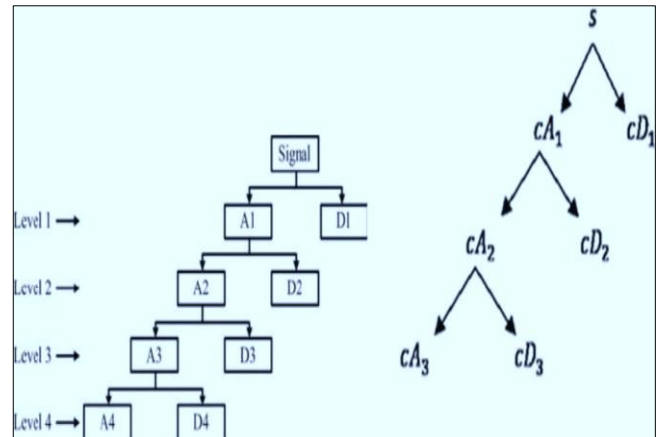


Figure 4. Signal decomposition using DWT

IV. CLASSIFICATION

A model for detecting pathological signals is developed utilizing the Adaptive Neuro Fuzzy Inference System (ANFIS). The predictive classification model is constructed by utilizing a dataset consisting of 100 normal and pathological signals obtained from the PhysioNet-Challenge 2016 in Cardiology Challenge dataset for training and testing purposes. Feature extraction is performed on each PCG signal of the database using Mel-scaled power spectrogram and mel-frequency cepstral coefficients (MFCC). Subsequently, these features are inputted into a deep neural network for model training with tensor flow. The model achieves an overall classification accuracy exceeding 84%. Hence,

this model can serve as an effective and reliable method for automatically differentiating between normal and abnormal heart sounds. The classification model's various steps are illustrated in Figure 5.

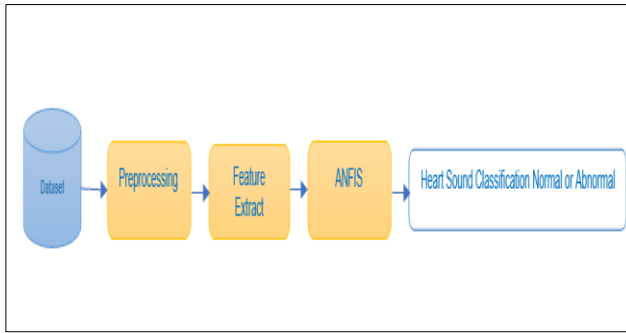


Figure 5. diagram of the proposed method

V. ADAPTIVA NEURO FUZZY INFERENCE SYSTEM (ANFIS)

The ANFIS classifier is a method of artificial intelligence that is suggestive in nature when it comes to the classification of data. Within the ANFIS architecture, there are five layers of nodes that play a crucial role. These layers have been designed to conduct a comparison between the input signal and the knowledge that has been previously stored through training. While two of the layers within ANFIS are adaptive, the remaining layers are made up of fixed nodes as indicated by references [28] and [29]. The parameters introduced into ANFIS for processing include Mean, SD, VAR, and Entropy. In the context of ANFIS, the value of 1 is used to signify an abnormal output, whereas the value of 0 is employed to denote a normal output.

VI. FEATURE EXTRACTION

Relevant features were extracted from the preprocessed signal, enabling the classification of the signal as normal or abnormal. These features include mean, standard deviation (SD), variance (Var), and entropy. Mean: Represents an intermediary value denoting the central tendency of all signal values. Standard Deviation - SD: Quantifies the extent of dispersion exhibited by signal values in relation to the mean. Variance - Var: The standard deviation metric serves as an alternative indicator of the spread of data points. Entropy: Assesses the level of unpredictability or randomness inherent within the signal data. The process involves the examination of cardiac sound signals subsequent to their processing, whereby a variety of crucial statistical parameters such as mean, standard deviation, variance, and entropy are derived from the processed signal. These metrics are subsequently utilized for the purpose of distinguishing between a normal and pathological cardiac signal.

VII. EEPERIMENTAL WORK

The function diagram of the proposed approach is represented in Figure 6, which consisted of 6 stages. All

the steps of the proposed method are described in the following subsections.

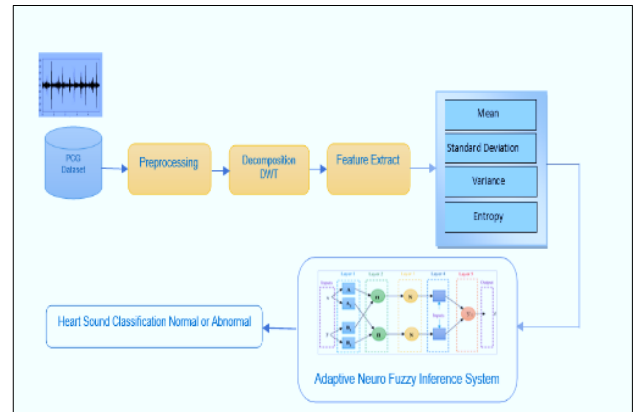


Figure 6 - Diagram Block of the purposed method

A. The Dataset

The dataset used in this study is part of the PhysioNet-Challenge 2016 [37] is a worldwide repository comprising over 3000 recordings. The duration of heart sound recording was about 10-60 seconds. The recordings are categorized into distinct classes denoted as A, B, C, D, E and F. A total of 1886 recordings were gathered from classes A, B, and E. These recordings were then partitioned into training and testing datasets of 80% and 20% respectively.

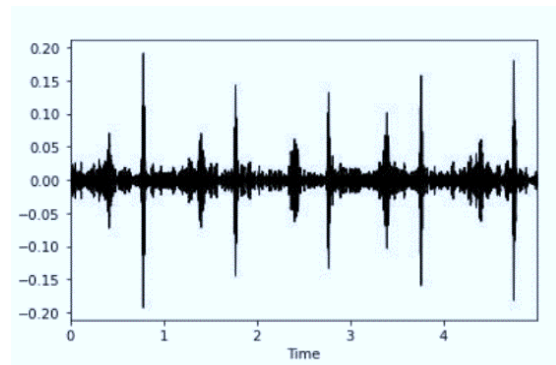


Figure 7 - PCG Signal from PhysioNet-Challenge 2016

B. Per-processing

The initial step involves preprocessing the cardiac sounds to produce the necessary Heart Sound data. During the preprocessing phase, the Heart Sound data undergoes normalization, filtering, and feature extraction. The normalization process is mathematically defined by the equation $x(n) = \frac{xr(n) - xr(\min)}{xr(\max) - xr(\min)}$ (1), where $xr(n)$ represents the recorded PCG signal and $x(n)$ signifies the normalized Heart Sound signal [40]. Additionally, $xr(\min)$ and $xr(\max)$ denote the minimum and maximum values of the Heart Sound, respectively. Subsequently, in the filtering stage, second-order high-pass and low-pass Butterworth filters with cut-off frequencies of 15 Hz and 700 Hz are utilized to filter the normalized PCG signal and eliminate undesired background noise.

VIII. RESULTS AND DISCUSSION

The precision, recall, and F1-score are metrics utilized for evaluating the performance of a classifier during testing. These metrics are calculated based on the classifier's true positive (TP), true negative (TN), false positive (FP), and false negative (FN) values. A confusion matrix is employed to ascertain the classifier's performance, as illustrated in Figure 8. To evaluate the performance of the system, statistical metrics such as PRECISION and RECALL are calculated using "equations (3), (4), and (5) ".

$$\text{Precision} = \frac{TP}{TP + FP} \tag{3}$$

$$\text{RECALL} = \frac{TP}{TP + FN} \tag{4}$$

$$\text{F-score} = \frac{2 * \text{precision} * \text{RECALL}}{\text{precision} + \text{RECALL}} \tag{5}$$

where:

TP: true positive represents the abnormal samples detected correctly

FP: false positive represents the normal samples detected as abnormal.

TN: true negative represents the normal samples detected correctly.

FN: false negative represents the abnormal samples detected as normal.

The confusion matrix is used to classify heart disease, where rows are natural and columns represent expected categories. Country cells indicate the number of accurate predictions. In this case, 225 predictions were made for individuals without (Normal) and 89 for those with (Abnormal). The binary classification model showed higher accuracy in determining heart disease.

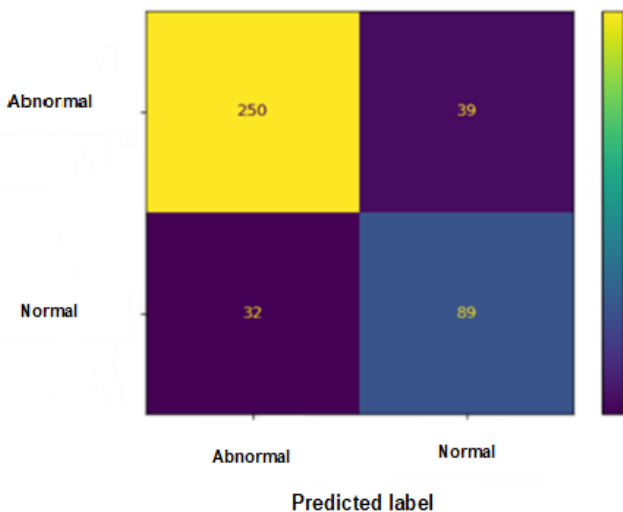


Figure 8. confusion matrix

In Figure 9 the y-axis shows the recall, which is the proportion of positive cases that were correctly identified by the model.

The x-axis shows the precision, which is the proportion of the model's positive identifications that were actually correct.

The curve in the plot shows the trade-off between recall and precision for different classification thresholds. As the threshold for classifying something as positive

increases, the precision will increase (because the model is being more careful about classifying things as positive), but the recall will decrease (because the model is missing more actual positive cases).

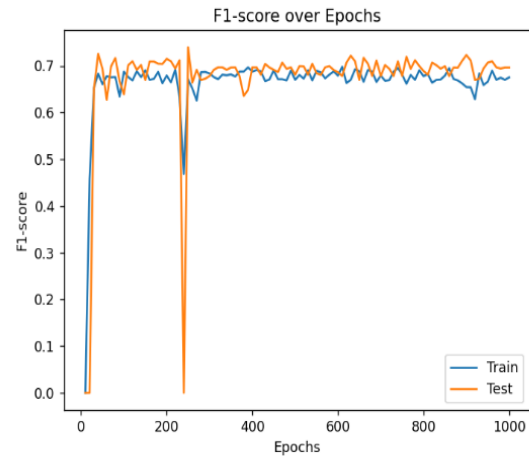


Figure 9 F1-score over Epochs

The training and testing performance was evaluated using a training and testing dataset. The figure 10 shows Recall trends were across epochs for both datasets, quantifying the model's ability to correctly identify positive cases.

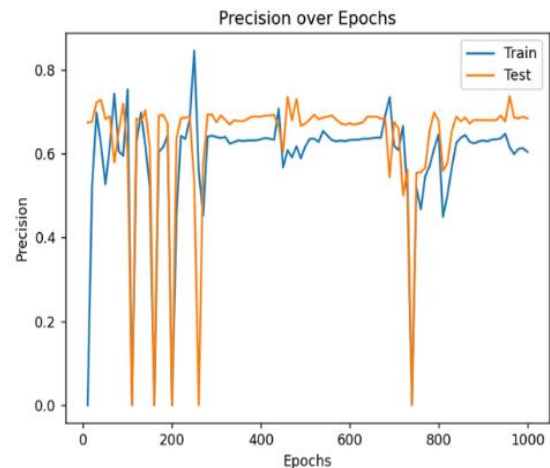


Figure 10. The training and testing performance (Precision)

Training and assessment efficacy were assessed utilizing a training set and a testing set. The Figure 11 illustrates the retrieval performance across different age groups for both the training set (depicted by the red line) and the testing set (depicted by the blue line). Recall serves as a metric for ascertaining the percentage of positive instances correctly distinguished by the model, specifically referring to accurately classified abnormalities in heart sounds. The recall typically rises as the quantity of agreements for both datasets increases, indicating an enhancement in the training and assessment efficacy of the training data and its capacity to detect irregularities in heart sounds. Nonetheless, it was observed that the recall rate on the testing set (Blue Line) consistently lagged behind that of the training set (Red Line). This discrepancy in performance is deemed highly appropriate.

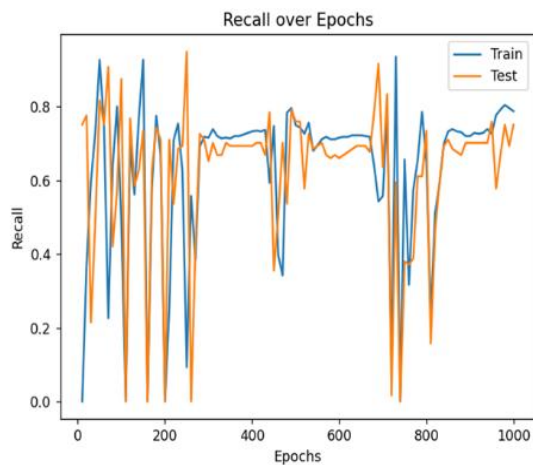


Figure 11. The training and testing performance (Recall Over Epochs)

In this manuscript, a machine learning technique known as Adaptive Neuro-Fuzzy Inference System (ANFIS) was applied for the purpose of identifying the auditory signals of the cardiac organ, distinguishing between normal and abnormal rhythms. The effectiveness of ANFIS was assessed through the utilization of distinct sets of data for training and testing. The graphical representation illustrates the variations in error rates across different stages of development for both the training set (depicted by the red line) and the test set (depicted by the blue line). Error, in this context, serves as a metric for evaluating the extent to which ANFIS-generated forecasts align with the actual categorization of cardiac sounds, whether they are normal or abnormal. Lower error values are indicative of superior performance by the ANFIS model. Generally, the error rate exhibits a decline with the progression of development stages for both the training and testing datasets, suggesting that the model acquires knowledge from the training data and enhances its capacity to make precise distinctions regarding abnormal cardiac sounds. It was observed that the error rate in the training dataset (red line) consistently converges towards a lower threshold in comparison to the test dataset (blue line) across various developmental stages. This disparity in performance levels alludes to the presence of an excessive degree of fitting. Figure 12.

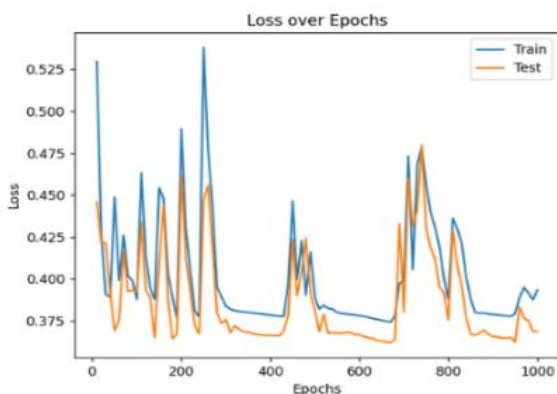


Figure 12. Loss Over Epochs for Machine Learning (ANFIS) Training

IX. CONCLUSION

This study explores the intricacies of feature extraction techniques, preprocessing approaches, and ANFIS-based classification methodologies utilizing Discrete Wavelet Transform (DWT). The results for classifying normal or abnormal heart sounds achieved an accuracy of 84%, with sensitivity ranging from 63% and specificity from 62%. These features demonstrate reliability in contributing to neural network systems for classifying cardiac sound signals. The combination of ANFIS and DWT attributes proves to be a valuable tool, effectively participating in the PhysioNet Challenge 2016.

X. REFERENCE

- [1] Rangayyan, R.M and Lehner, R.J. (1988). A review. *CRC Critical Reviews in Biomedical Engineering* 15 (3), 211-236.
- [2] Rangayyan, R.M And Lehner, R.J (1988). Phonocardiogram signal analysis: a review. *CRC Critical Reviews in Biomedical Engineering* 15 (3), 211-236.
- [3] Feigen, L.P (1971). Physical characteristics of sound and hearing. *American journal of Cardiology*, 28 (2), 130-133.
- [4] Tuteur, F.B (1988). Wavelet Transforms in signal detection. *IEEE ICASSP*, CH2561-9, 1435-1438.
- [5] Grossmann, A.; Holschneider, K.; Kronland-Martinet, R. and Morlet, J. (1987). Detection of abrupt changes in sound signal with the help of the wavelet transform. In: *Inverse problems: An interdisciplinary study*. Advances in Electronics and Electron physics. Supplement 19 [New York, Academic], 298-306
- [6] Obaidat, M.S. Phonocardiogram signal analysis: techniques and performance comparison. *Journal of Medical Engineering & Technology*, vol 17, No 6 (1993), 221-227.
- [7] Boashas, B (1993). Time-frequency signal analysis. In *Advances in spectrum Estimation*, edited by S. Haykin, (NJ: Prentice-Hall).
- [8] William J. Williams. (1997). Time-frequency and wavelets in Biomedical Signal Processing. Edited by METIN AKAY. *IEEE Press Serie in BME*. 3-8.
- [9] Olivier, R and Duhamel, P. Fast algorithms for Discrete and Continuous Wavelet Transforms. *IEEE Transactions Information Theory*, vol 38, No. 2, (1992), 569-586.
- [10] Harris, A., Sutton, G. and Towers, M. (1976). Physiological and clinical aspects of cardiac
- [11] Ren, Zhao, et al. (2023), "A comprehensive survey on heart sound analysis in the deep learning era." *arXiv preprint arXiv:2301.09362*.
- [12] Yamashita, Kyohei, et al. (2024) "Analysis of Unique Motility of the Unicellular Green Alga *Chlamydomonas reinhardtii* at Low Temperatures down to -8° C." *Micromachines* 15.3 :410.
- [13] Bao, Xinqi, and Yansha Deng. 2023, *Processing of Cardiac Signals for Health Monitoring and Early Detection of Heart Diseases*. Diss. King's College London.
- [14] Davidsen, Anne Herefoss, et al. (2023) "Diagnostic accuracy of heart auscultation for detecting valve disease: a systematic review." *BMJ open* 13.3: e068121.
- [15] Cheung, Yiu-fai. (2023), *Congenital and Paediatric Acquired Heart Disease in Practice*. Springer Nature.

- [16] Milani, M. M., Abas, P. E., & De Silva, L. C. (2022). A critical review of heart sound signal segmentation algorithms. *Smart Health*, 24, 100283.
- [17] Dubnov, S., & Greer, R. (2023). *Deep and shallow: Machine learning in music and audio*. CRC Press.
- [18] Omarov, B., Tuimebayev, A., Abdrakhmanov, R., Yeskarayeva, B., Sultan, D., & Aidarov, K. (2023). Digital stethoscope for early detection of heart disease on phonocardiography data. *International Journal of Advanced Computer Science and Applications*, 14(9).
- [19] Abbas, A. K., & Bassam, R. (2022). *Phonocardiography signal processing*. Springer Nature.
- [21] Abbas, S., Ojo, S., Al Hejaili, A., Sampedro, G. A., Almadhor, A., Zaidi, M. M., & Kryvinska, N. (2024). Artificial intelligence framework for heart disease classification from audio signals. *Scientific Reports*, 14(1), 3123.
- [22] Bao, X., Xu, Y., & Kamavuako, E. N. (2022). The effect of signal duration on the classification of heart sounds: A deep learning approach. *sensors*, 22(6), 2261.
- [23] Israr, M., Zia, M., Ur Rehman, N., Ullah, I., & Khan, K. (2023). Classification of normal and abnormal heart by classifying PCG signal using MFCC coefficients and CGP-ANN classifier. *Mehran University Research Journal Of Engineering & Technology*, 42(3), 160-166.
- [24] Torre-Cruz, J., Martínez-Muñoz, D., Ruiz-Reyes, N., Muñoz-Montoro, A. J., Puentes-Chiachio, M., & Cañadas-Quesada, F. J. (2022). Unsupervised detection and classification of heartbeats using the dissimilarity matrix in PCG signals. *Computer Methods and Programs in Biomedicine*, 221, 106909.
- [25] Chowdhury, T. H., Poudel, K. N., & Hu, Y. (2020). Time-frequency analysis, denoising, compression, segmentation, and classification of PCG signals. *Ieee Access*, 8, 160882-160890.
- [26] Guo, N., Si, X., Zhang, Y., Ding, Y., Zhou, W., Zhang, D., & Hong, B. (2021). Speech frequency-following response in human auditory cortex is more than a simple tracking. *Neuroimage*, 226, 117545.
- [27] Al, E., Stephani, T., Engelhardt, M., Haegens, S., Villringer, A., & Nikulin, V. V. (2023). Cardiac activity impacts cortical motor excitability. *PLoS Biology*, 21(11), e3002393.
- [28] Aburakhia, S., Shami, A., & Karagiannidis, G. K. (2024). On the Intersection of Signal Processing and Machine Learning: A Use Case-Driven Analysis Approach. *arXiv preprint arXiv:2403.17181*.
- [29] Potdar, R. M. (2021). Optimal parameter selection for DWT based PCG denoising. *Turkish Journal of Computer and Mathematics Education (TURCOMAT)*, 12(9), 3507-3519.
- [30] Daud, S. N. S. S., & Sudirman, R. (2022). Wavelet based filters for artifact elimination in electroencephalography signal: A review. *Annals of Biomedical Engineering*, 50(10), 1271-1291.
- [31] Moradi, M. (2022). Wavelet transform approach for denoising and decomposition of satellite-derived ocean color time-series: Selection of optimal mother wavelet. *Advances in Space Research*, 69(7), 2724-2744.
- [32] Chen, G., Li, K., & Liu, Y. (2021). Applicability of continuous, stationary, and discrete wavelet transforms in engineering signal processing. *Journal of Performance of Constructed Facilities*, 35(5), 04021060.
- [33] Zhilyakov, E. G., Belov, S. P., Oleinik, I. I., Babarinov, S. L., & Trubitsyna, D. I. (2020). Generalized sub band analysis and signal synthesis. *Bulletin of Electrical Engineering and Informatics*, 9(3), 964-972.
- [34] Babalola, O. P., & Versfeld, J. (2024). Wavelet-based feature extraction with hidden Markov model classification of Antarctic blue whale sounds. *Ecological Informatics*, 80, 102468.
- [35] Achmamad, A., & Jbari, A. (2020). A comparative study of wavelet families for electromyography signal classification based on discrete wavelet transform. *Bulletin of Electrical Engineering and Informatics*, 9(4), 1420-1429.
- [36] Kankanamge, Y., Hu, Y., & Shao, X. (2020). Application of wavelet transform in structural health monitoring. *Earthquake Engineering and Engineering Vibration*, 19, 515-532.
- [37] Al-Naami, B., Fraihat, H., Gharaibeh, N. Y., & Al-Hinnawi, A. R. M. (2020). A framework classification of heart sound signals in PhysioNet challenge 2016 using high order statistics and adaptive neuro-fuzzy inference system. *IEEE Access*, 8, 224852-224859.
- [40] Roy, T. S., Roy, J. K., Mandal, N., & Mukhopadhyay, S. C. (2024). Recent Advances in PCG Signal Analysis using AI: A Review. *International Journal on Smart Sensing and Intelligent Systems*, 17(1).